Coordination-induced switch between the singly occupied and the lowest unoccupied molecular orbitals in two methylviologen-derived chromophores

Eberhard Waldhör,[a] Mthembeni M. Zulu,[b] Stanislav Zalis[c] and Wolfgang Kaim*,[a]

[a] *Institut für Anorganische Chemie der Universität, Pfaffenwaldring 55, D-70550 Stuttgart, Germany*
[b] *Department of Chemistry, University of the Zululand, Private Bag X1001, Kwa-Dlangezwa 3886, South Africa*
[c] *J. Heyrovsky Institute of Physical Chemistry, Academy of Sciences of the Czech Republic, Dolejškova 3, CZ-18223 Prague, Czech Republic*

The aromatic heterocycles 2,7-diazapyrene (dap) and 3,6-bis(4-pyridyl)-1,2,4,5-tetrazine (4-bptz) each exhibit two very close-lying lowest unoccupied molecular orbitals (MOs) with very different character, *viz.*, a methylviologen-like† MO (b_{1u}) and a quinonoid (dap) or tetrazine-localized MO (4-bptz) of a_u symmetry. Calculations (HMO, semiempirical NDO type, *ab initio*) suggest that the orbital crossing between b_{1u} and a_u and thus the character of the singly occupied MO in one-electron reduced compounds can be effected by removal of electron density from the potentially coordinating pyridyl nitrogen centres. We have explored this suggestion experimentally by coordination of electrophiles, either alkyl cations, R^+, or neutral complex fragments, $W(CO)_5$, to both pyridine N centres. Experimental data from UV–VIS–NIR and especially EPR spectroelectrochemistry show that coordination of two neutral $W(CO)_5$ fragments to dap is sufficient to cause a change from singly occupied a_u (in $dap^{\cdot-}$) to singly occupied b_{1u} in $\{dap[W(CO)_5]_2\}^{\cdot-}$. In contrast, the $4\text{-}bptz^{\cdot-}$ radical system requires coordination of two electrophiles R^+ ($R = CH_3, C_2H_5$) in order to move b_{1u} below a_u while the ditungsten(0) radical anion complex is still a ^2A_u species.

Low-lying unoccupied π molecular orbitals (π*) are essential for many physical and chemical characteristics of conjugated π systems and their complexes. Electron uptake in the ground state (reduction) or excitations to π→π*, n→π* or to $d_\pi \rightarrow \pi^*$ (charge transfer) excited states involve an at least temporary occupation of such orbitals, their nature determining the structure and reactivity of the corresponding states. In most instances, there is no question as to which the lowest-lying π* MO in small or intermediate-size molecular π systems is because even elementary Hückel MO calculations usually give unequivocal answers.[1] However, there may be situations where, in the absence of actual orbital degeneracy, two different low-lying MOs can compete for the distinction of being the lowest unoccupied MO, the LUMO.

One of the best established examples for such a situation is the common chelate ligand 1,10-phenanthroline (phen) for which various kinds of calculations predict close-lying b_1 and a_2 orbitals as the LUMO or second-lowest unoccupied MO (SLUMO), respectively.[2] An EPR study of one-electron reduced phen has shown that the b_1 MO with high spin density at the potentially coordinating nitrogen centres is being occupied by the single electron in all instances observed.[2a]

In the course of designing new π-conjugated bridging ligands[3] and surveying established systems for their suitability to promote metal–metal interaction *via* n donor centre-containing π systems, we found two molecules derived from the 4,4′-bipyridine structure in which different degrees of external perturbation cause a significant change in the type of singly occupied MO (SOMO) after reduction.

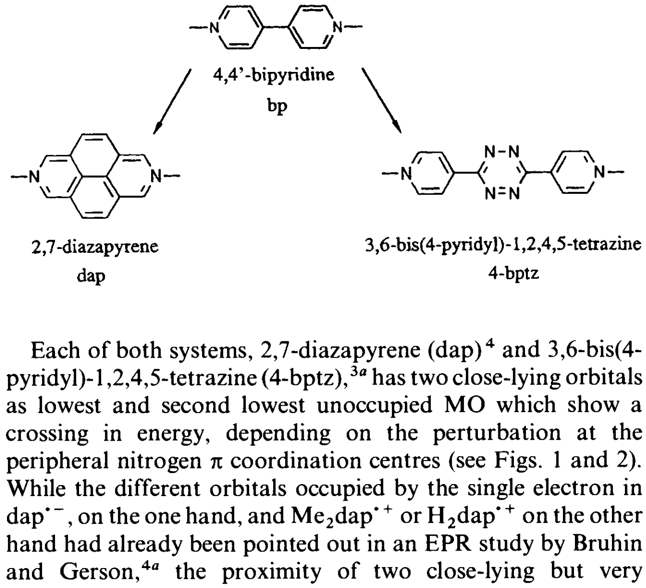

4,4′-bipyridine
bp

2,7-diazapyrene
dap

3,6-bis(4-pyridyl)-1,2,4,5-tetrazine
4-bptz

Each of both systems, 2,7-diazapyrene (dap)[4] and 3,6-bis(4-pyridyl)-1,2,4,5-tetrazine (4-bptz),[3a] has two close-lying orbitals as lowest and second lowest unoccupied MO which show a crossing in energy, depending on the perturbation at the peripheral nitrogen π coordination centres (see Figs. 1 and 2). While the different orbitals occupied by the single electron in $dap^{\cdot-}$, on the one hand, and $Me_2dap^{\cdot+}$ or $H_2dap^{\cdot+}$ on the other hand had already been pointed out in an EPR study by Bruhin and Gerson,[4a] the proximity of two close-lying but very different unoccupied MOs for 4-bptz was mentioned in a study of ditungsten(0) complexes.[3a] We now present a theoretical and experimental study of these systems, exploring (*i*) whether weak electrophiles such as $W(CO)_5$ can already cause an orbital switch in $dap^{\cdot-}$ and (*ii*) whether the b_{1u} MO can be singly occupied in $4\text{-}bptz^{\cdot-}$ after coordination of strongly electrophilic alkyl cations R^+ ($R = CH_3$ or C_2H_5).

Spectroelectrochemical studies (EPR, UV–VIS–NIR) have been used to investigate known compounds such as $Me_2dap^{2+/\cdot+}$ and $\{(4\text{-}bptz)[W(CO)_5]_2\}^{0/\cdot-}$ as well as new species, *i.e.* the dinuclear complex $\{(dap)[W(CO)_5]_2\}^{0/\cdot-}$ and the methylviologen derivatives $R_2(4\text{-}bptz)^{2+/\cdot+/0}$ (R = Me, Et).

---

† IUPAC name for methylviologen is 1,1′-dimethyl-4,4′-bipyridinium.

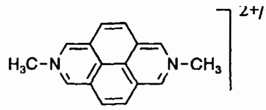

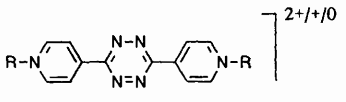

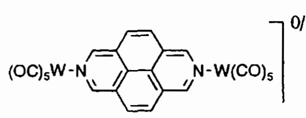

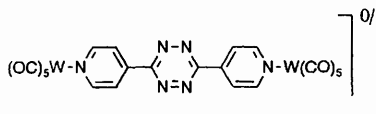

Experimental

Syntheses

All experiments were performed under an argon atmosphere using dried solvents. The compounds dap, $Me_2dap(BF_4)_2$ and (4-bptz)$[W(CO)_5]_2$ were obtained according to literature procedures.[3a,4,5]

(μ-dap)$[W(CO)_5]_2$. Two equiv. $W(CO)_6$ (141 mg, 0.40 mmol) were irradiated in *ca.* 150 cm^3 tetrahydrofuran (THF) under UV light to yield the yellow solution of the solvate (THF)$W(CO)_5$ according to standard procedures. This solution was then allowed to react at room temperature with one equiv. dap (41 mg, 0.20 mmol) for 15 h. After removal of the solvent the yellow product was recrystallized from THF–toluene (1 : 1). Subsequent treatment for 4 h under vacuum at ambient temperature served to remove $W(CO)_6$ by sublimation to yield 150 mg (87%) of the yellow product (Found: C, 33.2; H, 1.0; N, 3.0. $C_{24}H_8N_2O_{10}W_2$ requires C, 33.83; H, 0.95; N, 3.29%); δ_H(CDCl$_3$) 8.27 (4 H, s, 4,5,9,10-H) and 9.73 (4 H, s, 1,3,6,8-H); ν_{max}(CH$_2$Cl$_2$)/cm^{-1} (CO) 2071 (s), 1980 (w), 1937 (vs) and 1906 (sh).

[Me_2(4-bptz)]$(BF_4)_2$. A mixture of 95 mg (0.40 mmol) 4-bptz and 133 mg (0.90 mmol) Me_3OBF_4 was heated to reflux in 40 cm^3 acetonitrile for 18 h. After reducing the volume to *ca.* 3–5 cm^3 an amount of 10 cm^3 1,2-dichloroethane was added and the solution was cooled to -28 °C. Filtration under argon yielded 120 mg (68%) of a bright red material (Found: C, 38.1; H, 3.4; N, 18.4. $C_{14}H_{14}B_2F_8N_6$ requires C, 38.22; H, 3.21; N, 19.10%); δ_H[(CD$_3$)$_2$CO] 4.80 (6 H, s, Me), 9.18 (4 H, m, 3,3′,5,5′-H) and 9.42 (4 H, m, 2,2′,6,6′-H).

[Et_2(4-bptz)]$(PF_6)_2$. A mixture of 60 mg (0.25 mmol) 4-bptz and 155 mg (0.62 mmol) Et_3OPF_6 was heated to reflux in 50 cm^3 1,2-dichloroethane for 20 h. Filtration and drying of the precipitate which formed after cooling yielded 92 mg (63%) of a light red compound (Found: C, 32.3; H, 3.0; N, 14.1. $C_{16}H_{18}F_{12}N_6P_2$ requires C, 32.89; H, 3.11; N, 14.38%); δ_H[(CD$_3$)$_2$CO] 1.88 (6 H, t, CH$_3$), 5.11 (4 H, q, CH$_2$), 8.80 (4 H, m, 3,3′,5,5′-H) and 9.50 (4 H, m, 2,2′,6,6′-H).

Singly and, in some instances, doubly reduced forms were obtained by various methods. The radical anions $dap^{\bullet -}$ and ($dap^{\bullet -}$)$[W(CO)_5]_2$ were generated for EPR–ENDOR and UV–VIS spectroscopy by reduction with distilled potassium metal in THF solution. Radical cations $Me_2dap^{\bullet +}$ and R_2(4-bptz)$^{\bullet +}$ (R = Me, Et) were generated for study by EPR and UV–VIS–NIR spectroscopies by reduction with thallium metal in dimethylformamide (DMF) or by cathodic reduction in DMF–0.1 mol dm^{-3} Bu_4NPF_6 in a two-electrode cell.[6a] Otherwise, an optically transparent thin-layer electrode (OTTLE) cell was used for UV–VIS–NIR spectroelectrochemistry.[6b]

Instrumentation

EPR and ENDOR spectra were recorded in the X-band on a Bruker System ESP 300 equipped with an ENI A500 RF amplifier, a Bruker ER033 field frequency lock, a Bruker ER035M gaussmeter and a HP 5350B microwave counter. NMR spectra were recorded on a Bruker AM 250 spectrometer, IR vibrational spectra were recorded on Perkin-Elmer instruments 684 and 283. Spectrophotometers Shimadzu UV160 and Bruins Instruments Omega 10 were used to record UV–VIS–NIR absorption spectra. Emission spectra were obtained on a Perkin-Elmer LS-3B instrument. Cyclic voltammetry was carried out using a three-electrode configuration (glassy carbon working electrode, Ag/AgCl reference, Pt wire) and a PAR 273/175 potentiostat and function generator. Dry solvents were used with 0.1 mol dm^{-3} Bu_4NPF_6 as electrolyte; for studies of R_2(4-bptz)$^{\bullet +}$ (R = Me, Et), a solution pre-reduced with thallium was used.

Calculations

Ab initio calculations were performed using the GAUSSIAN 92[7a] program package. The 6-31G basis was used for geometry optimization of neutral systems with D_{2h} or C_{2v} symmetry. The optimized geometries of open shell systems were calculated using the restricted and unrestricted HF approach with a 3-21G basis set. For molecules that contain adjacent heteroatoms with electron pairs a basis set having polarization functions is preferred. Therefore, comparable calculations with a 6-31** basis set were performed for 1,2,4,5-tetrazine (tz), 1,4-dihydro-1,2,4,5-tetrazine(tzH_2) and $tz^{\bullet -}$. Test calculations using the limited basis mentioned above indicated that the trends in bond length variations and orbital energy sequences were not significantly influenced by exclusion of polarization functions. The programs for HMO perturbation and for semiempirical MNDO and AM1 calculations were used as available.[1b,7b,c] The INDO/S method[7d] followed by configuration interaction (CI) was used for calculating electronic transitions.

Results and discussion

Calculations

Theoretical studies were carried out at various levels for different oxidation states of the heterocycles and their diquaternized forms. These calculations include Hückel MO theory for establishing trends in orbital energies and for spin population calculations, AM1 semiempirical and *ab initio* methods for geometry optimization and for the determination of exact orbital sequences, and INDO/S + CI procedures for the calculation of electronic transition energies and intensities. No calculations were done on the dinuclear tungsten complexes which were treated within a perturbation approach.[2a] Identification of the MOs involved and a perturbation treatment of the orbital sequence are already possible using the elementary Hückel MO approach.[1] Fig. 1(*a*) shows the response of Hückel π MO energies as a function of the Coulomb integral parameter h_N at the peripheral nitrogen coordination centres in the case of dap; Fig. 2 gives a representation of the low-lying MOs competing for the role of the LUMO. In both dap and 4-bptz π systems, the a_u MO is the LUMO for small values of h_N, in particular for $h_N = h_C = 0.0$. Stronger stabilization of the b_{1u} orbital causes an orbital reversal a_u/b_{1u} at perturbation values h_N which are in the standard range for heteroatom parameters,[1a,b] *i.e.* at h_N *ca.* 1.06 for 4-bptz and at h_N *ca.* 1.45 for dap [Fig. 1(*a*)].

Naturally, the calculated π spin populations ρ_π using the Hückel MO–McLachlan approximation[8] also depend on the choice of h_N; the data were converted to calculated EPR coupling constants *via* McConnell-type equations [eqn. (1)] and are summarized together with the experimental results

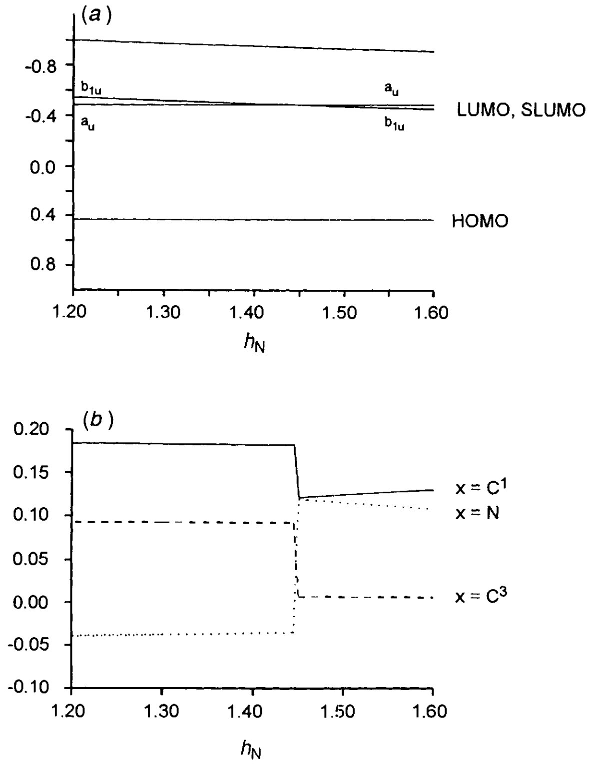

Fig. 1 (*a*) Frontier molecular orbital energies α of dap as a function of the Coulomb integral perturbation parameter h_N ($h_C = 0.0$, $k_{CC} = k_{CN} = 1.0$). (*b*) Calculated HMO–McLachlan π spin populations $\rho_\pi(x)$ for dap$^{\bullet-}$ as a function of h_N ($\lambda = 1.2$).

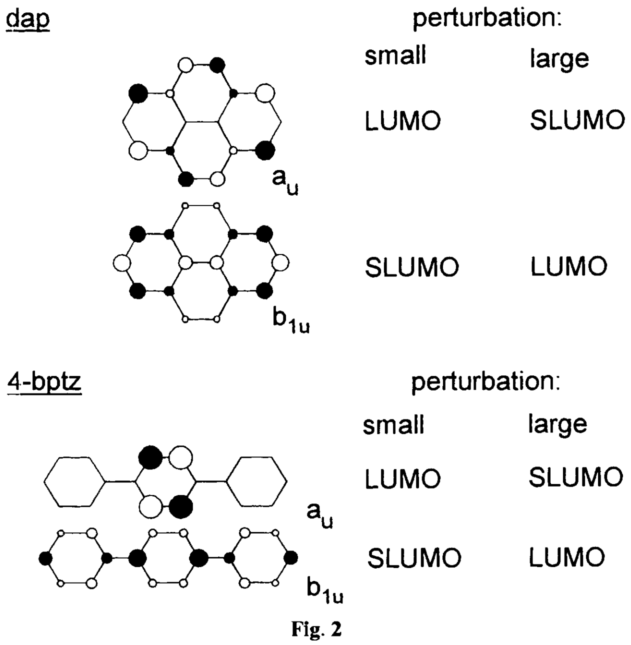

Fig. 2

(*vide infra*) in Table 1. For the one-electron reduced dap$^{\bullet-}$ system, the perturbation diagram in Fig. 1(*b*) illustrates a stark discontinuity of the π spin distribution at the orbital crossing point.

Application of the *ab initio* method to the neutral dap molecule with optimized geometry (D_{2h}) shows that the lowest unoccupied MO is of a_u character. Introduction of two methyl groups at the nitrogen centres causes a reversal of the LUMO/SLUMO order, $E(b_{1u}) < E(a_u)$, as predicted similarly by the HMO method [Fig. 1(*a*)]. Calculations on reduced species yield the previously suggested ^2A_u ground state for dap$^{\bullet-}$ and a $^2B_{1u}$ ground state for Me$_2$dap$^{\bullet+}$.[4a] Semiempirical and *ab initio* methods essentially lead to the same results. Both radical ions are calculated to have significantly non-planar structures in terms of a saddle-shaped arrangement, a result which may account for some discrepancies between experimental and HMO-calculated values (Table 1). In a similar vein, doubly reduced phenanthrene was recently calculated by *ab initio* methods to have a non-planar energy minimum structure.[9]

$$a = \rho_\pi Q \tag{1}$$

[Q_{CH} = 2.3 mT, Q_N = 2.76 mT (pyridine-N)[8] or 1.70 mT (tetrazine-N).]

Semiempirical calculations of the tetrazine system turned out to be difficult because it was not possible to describe the geometry correctly by these methods. However, the *ab initio* method using a 6-31G basis set yielded almost equidistant C–N and N–N bond lengths of 133.0 and 131.8 pm, respectively, within the tetrazine ring. For comparison, the crystal structure of unsubstituted 1,2,4,5-tetrazine revealed values of 133.4 and 132.1 pm, respectively.[10a] The *ab initio* calculation gives an almost degenerate set of unoccupied a_u and b_{1u} molecular orbitals. In contrast to the a_u orbital, the b_{1u} orbital is stabilised by inter-aryl π delocalization. Rotation around the inter-aryl bonds (147 pm) in 4-bptz thus shifts the b_{1u} orbital to higher energies and enlarges the separation between these orbitals. Calculations of Me$_2$(4-bptz)$^{2+}$ illustrate the orbital switch by revealing b_{1u} as the LUMO.

The calculations on reduced species yield the ^2A_u ground state for 4-bptz$^{\bullet-}$ and a $^2B_{1u}$ ground state for Me$_2$(4-bptz)$^{\bullet+}$, as in the case of the dap systems. The optimized geometry of 4-bptz$^{\bullet-}$ is characterized by C–N, N–N and inter-ring C–C bond lengths of 141, 132 and 149 pm, respectively. These values reproduce rather well the geometry which had been determined experimentally for a dicopper(I) derivative of 3,6-bis(2-pyridyl)-1,2,4,5-tetrazine radical anion (2-bptz$^{\bullet-}$). The intra-tetrazine distances for {(μ-2-bptz)[Cu^I(PPh$_3$)$_2$]$_2$}(BF$_4$) are $d_{N\text{-}N}$ 139.9(10), $d_{C\text{-}N}$ 130.2(8) and $d_{C\text{-}N(\text{-}Cu)}$ 133.9(10) pm.[10b,c] In agreement with conventional notation, the geometry of Me$_2$(4-bptz)$^{\bullet+}$ is characterized by a quinonoid structure with $d_{N\text{-}N}$ 128, $d_{C\text{-}N}$ 137 pm and short inter-ring distances $d_{C\text{-}C}$ at 142 pm.

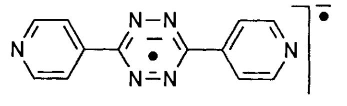

4-bptz$^{\bullet-}$

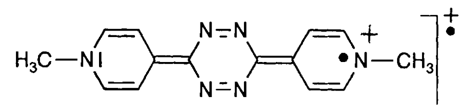

R$_2$(4-bptz)$^{\bullet+}$

The electronic spectra were calculated using the spectrally parametrized INDO/S method[7c] and the optimized geometries as referred to above. Table 2 summarizes calculated and experimental data.

Electrochemistry

All compounds investigated undergo at least one reversible one-electron reduction to a paramagnetic species (Table 3). Whereas the reduction of the dap systems proceeds at fairly negative potentials, the compounds involving 4-bptz are reduced rather easily. However, the response of the ligand-centred reduction to coordination by W(CO)$_5$ or R$^+$ is much more pronounced for the dap system with its appreciable π LUMO coefficients at the coordinating nitrogen sites (Fig. 2). The much more limited response of 4-bptz can be attributed to a dominant role of the a_u orbital and/or rather small MO coefficients at the pyridyl nitrogen centres of the b_{1u} MO (Fig. 2).

The particularly small change of E_{red1} between 4-bptz and its ditungsten(0) complex has been interpreted as a consequence of

Table 1 EPR data of radical species

Radical	g	$a(^{14}\mathrm{N})$/mT	$a(^{1}\mathrm{H})$/mT	$a(^{183}\mathrm{W})$/mT	Solvent
dap$^{\bullet -}$ (exp.)[a]	2.0027	0.157	0.505 (H^1), 0.215 (H^3)	—	THF
dap$^{\bullet -}$ (calc.)[b]	—	0.125	0.428 (H^1), 0.213 (H^3)	—	—
(dap$^{\bullet -}$)[W(CO)$_5$]$_2$	2.0052	0.458	0.166 (H^1), 0.025 (H^3)	0.139	THF
Me$_2$dap$^{\bullet +}$ (exp.)	na	0.470	0.183 (H^1), 0.040 (H^3)	—	CH$_3$OH
Me$_2$dap$^{\bullet +}$ (calc.)[b]	—	0.319	0.287 (H^1), 0.014 (H^3)	—	—
bptz$^{\bullet -}$ (exp.)[c]	2.0040	0.493 (tz)	<0.03	—	CH$_2$Cl$_2$
bptz$^{\bullet -}$ (calc.)[b]	—	0.505 (tz)	<0.03	—	—
(bptz$^{\bullet -}$)[W(CO)$_5$]$_2$[c]	2.0039	0.488 (tz)	<0.03	<0.05	CH$_2$Cl$_2$
Me$_2$bptz$^{\bullet +}$ (exp.)	2.0024	0.043 (tz)[d]	*d*	—	DMF
Me$_2$bptz$^{\bullet +}$ (calc.)[b]	—	0.032 (tz)	0.115 (H^2), 0.078 (H^3), 0.185 (N$_{py}$)	—	—

[a] From ENDOR spectroscopy at 250 K. [b] From HMO–McLachlan calculations, using $h_N = 0.90$ (anions), $h_N = 1.5$ (cations) and $\lambda = 1.2$ (ref. 8); $Q_{CH} = 2.3$ mT, $Q_N = 2.76$ mT for pyridine-N and $Q_N = 1.70$ for tetrazine-N. [c] From ref. 3*a*; tz, tetrazine. [d] Multiline spectrum (Fig. 3) with 0.043 mT as smallest coupling constant, attributed to tetrazine nitrogen centres.

Table 2 Absorption data[a,b] of compounds

Compound	λ/nm			Solvent
dap (exp.)	383 [10 600], 377 [4500], 363 [5900]; 334 [29 000], 319 [22 300], 307 [10 900] (sh)			THF
dap (calc.)	367 (0.120); HOMO→SLUMO	325 (0.712) HOMO→LUMO		
dap$^{\bullet -}$ (exp.)	1016 [830], 897 [680], 807 [480]; 712 [1550], 590 [1200]; 486 [8200], 447 [7800]; 403 [8000]; 384 [9200]			THF
dap$^{\bullet -}$ (calc.)	897 (0.048); SOMO→SLUMO	681 (0.011); SOMO→FLUMO[c]	501 (0.337) HOMO→SOMO	
dap[W(CO)$_5$]$_2$	450 [5900] (MLCT, sh); 401 [17 000] (LF); 336 [36 000], 325 [30 200] (sh)			THF
(dap$^{\bullet -}$)[W(CO)$_5$]$_2$	911 [6400], 830 [5700] (sh); 798 [7100]; 706 [8900]; 653 [10 600]; 639 [10 600], 587 [8400] (sh); 488 [19 100]; 441 [28 300]			THF
Me$_2$dap^{2+} (exp.)	418 [12 600], 393 [7400], 372 [2700]; 335 [29 700], 320 [19 500], 307 [7700]			CH$_3$CN
Me$_2$dap^{2+} (calc.)	422 (0.312); HOMO→LUMO	330 (0.439) HOMO→SLUMO[c]		
Me$_2$dap$^{\bullet +}$ (exp.)	771 [1500]; 685 [2700], 625 [3000], 580 [2700]; 445 [7000]			CH$_3$CN
Me$_2$dap$^{\bullet +}$ (calc.)	1123 (0.118); SOMO→LUMO	556 (0.059); SOMO→TLUMO	465 (0.093) HOMO→SOMO	
Me$_2$dap^{0} (exp.)	563 [6800]			CH$_3$CN
Me$_2$dap^{0} (calc.)	470 (0.613) HOMO→SLUMO			
bptz (exp.)	530 [450]			DMF
bptz (calc.)	467 (0.014) n→LUMO (π^*)			
bptz$^{\bullet -}$ (exp.)	510 [400] (br); 363 [21 500]; 344 [21 200]			DMF
bptz$^{\bullet -}$ (calc.)	560 (0.006); SOMO→SLUMO	467 (0.008); n→SOMO	324 several components	
(bptz)[W(CO)$_5$]$_2$	438 (sh, MLCT);	400 (LF)		DMF
(bptz$^{\bullet -}$)[W(CO)$_5$]$_2$	670 (br);	400 (LF)		DMF
Me$_2$bptz^{2+} (exp.)	526 [410];	290 [8200]		DMF
Me$_2$bptz^{2+} (calc.)	469 (0.010); n→LUMO	283 (1.460) HOMO→LUMO		
Me$_2$bptz$^{\bullet +}$ (exp.)	905 [5900], 809 [3000], 730 [650]; 525 [660] (sh); 460 [5700], 427 [5100], 400 [2500] (sh)			DMF
Me$_2$bptz$^{\bullet +}$ (calc.)	1017 (0.417); SOMO→LUMO 439 (0.011) SOMO→FLUMO	521 (0.000); SOMO→TLUMO	457 (1.073); HOMO→SOMO	
Me$_2$bptz^{0} (exp.)	763 [1300]; 639 [8700], 619 [8200] (sh); 433 [4600]			DMF
Me$_2$bptz^{0} (calc.)	598 (0.000); HOMO→SLUMO	561 (2.956); HOMO→LUMO	445 (0.018) n→SLUMO	

[a] Experimental absorption maxima from spectra recorded at room temperature (extinction coefficients ε in dm^3 mol^{-1} cm^{-1} in brackets); calculated values from INDO/S calculations (oscillator strengths in parentheses). [b] Bands related by vibrational structuring are separated by commas; bands belonging to different electronic transitions are separated by semicolons. [c] TLUMO and FLUMO: third and fourth lowest unoccupied molecular orbitals.

the electron addition to the a$_u$ MO in both species, a suggestion which was confirmed by EPR studies.[3a] The shift for E_{red1} between (4-bptz)[W(CO)$_5$]$_2$ and [R$_2$(4-bptz)]$^{2+}$ is about twice as large, which already indicates a qualitative change in the electronic structure. Such a change is also suggested by the appearance of a close-lying ($\Delta E = 0.2$ V) second reversible reduction wave of the *N,N′*-dialkylated compounds, which would be typical for a methylviologen-type or 'Weitz-type'[11a,b] redox system [R$_2$(4-bptz)]$^{n+}$ if b$_{1u}$ were the LUMO. In contrast, 1,2,4,5-tetrazine derivatives with a$_u$ as the LUMO are distinguished by large differences ($E_{\mathrm{red1}} - E_{\mathrm{red2}}$) > 0.8 V and often irreversible second reduction processes.[11c,d]

The difference between a$_u$ and b$_{1u}$ MOs is not as pronounced for the dap π system as for the 4-bptz species which precludes

Table 3 Electrochemical data[a] of compounds

Compound	E_{ox}/V	E_{red1}/V	E_{red2}/V	Solvent
dap		−2.54 (pc)		CH_2Cl_2
		−2.29 (110)		THF
dap$[W(CO)_5]_2$	+0.76 (pa)	−1.78 (90)		CH_2Cl_2
	+0.78 (pa)	−1.68 (97)	−2.00 (pc)	THF
Me_2dap^{2+}		−0.86 (94)	−1.42 (pc)	DMF
		−0.83 (81)	−1.42 (pc)	CH_3CN
4-bptz		−1.13 (70)		CH_2Cl_2
		−1.01 (90)	−2.46 (pc)	DMF
		−1.07 (54)		CH_3CN
(4-bptz)$[W(CO)_5]_2$	+0.76 (pa)	−0.92 (100)		CH_2Cl_2
		−0.95 (94)	−1.91 (pc)	DMF
$Me_2(4\text{-bptz})^{2+}$		−0.68 (80)	−0.91 (101)	DMF
$Et_2(4\text{-bptz})^{2+}$		−0.72 (88)	−0.88 (124)	DMF
		−0.61 (51)	−0.85 (96)	CH_3CN

[a] From cyclic voltammetry at 100 mV s^{-1} with 0.1 mol dm^{-3} Bu_4NPF_6 as electrolyte. Potentials in V *vs.* $Fc^{0/+}$, peak potential differences in mV (in parentheses); pc and pa are cathodic or anodic peak potentials for irreversible reduction or oxidation.

assignments based only on electrochemical data. All three species dap, (dap)$[W(CO)_5]_2$ and $[Me_2(dap)]^{2+}$ are reduced at similar values as corresponding derivatives with 4,4′-bipyridine[11a,12a] instead of dap as bridging ligand. Nevertheless, we could confirm by EPR–ENDOR spectroscopy the proposed[4a] occupation of a quinonoid MO (a_u) in the non-coordinated radical anion $dap^{\bullet -}$.

EPR–ENDOR Spectroscopy

An ENDOR spectrum of $dap^{\bullet -}$ and high-resolution EPR spectra of $[Me_2(dap)]^{\bullet +}$ allowed us to unambiguously analyse the ^1H and ^{14}N hyperfine coupling which, in connection with HMO–McLachlan calculated π spin populations, clearly confirms the difference between the singly occupied MOs in both radical ions (Table 1).[4a]

The question of what kind of MO would be the SOMO in the complex $(dap^{\bullet -})[W(CO)_5]_2$ was addressed here. Analysis of the EPR spectrum obtained from reduction of the neutral complex with potassium in THF gave a ^{14}N hyperfine splitting, a *g* factor and a ^{183}W isotope coupling (Table 1) which are very close to corresponding values of $(bp^{\bullet -})[W(CO)_5]_2$ (bp = 4,4′-bipyridine): $a(^{14}N)$ 0.433 mT, $a(^{183}W)$ 0.163 mT and *g* 2.0050.[13] Since it is clearly the b_{1u} MO that is singly occupied in the bp radical complex we assume the same here for the dap analogue. If the a_u MO with its small MO coefficients in the 2,7-position were singly occupied one would expect much smaller metal and nitrogen coupling constants and a *g* factor closer to the free electron value of $g = 2.0023$. We thus conclude that the reduced ditungsten(0) complex of dap has a $^2B_{1u}$ ground state like the dialkylated, methylviologen-analogous species, but different from the ^2A_u ground state of the free ion $dap^{\bullet -}$

This behaviour of the dap system contrasts with that of 4-bptz where previous EPR studies had shown no change in the SOMO when going from the ligand radical anion to its bis(pentacarbonyltungsten) complex.[3a] In both instances, simple nonets (Fig. 3) due to coupling of the four equivalent tetrazine nitrogen centres (^{14}N: $I = 1$) were observed at $g = 2.0040$, proving the occupation of a_u upon reduction. When reducing both dialkylated derivatives $R_2(4\text{-bptz})^{2+}$ to the radical cations, however, multiline spectra were obtained (Fig. 3) which could not be fully resolved due to extensive overlapping of hyperfine features. Such a spectrum is indeed expected for a $^2B_{1u}$ species, in which a total of 7875 theoretical lines (R = Me) would be expected from coupling with ^1H and ^{14}N nuclei. For the better resolved spectrum of $Me_2(4\text{-bptz})^{\bullet +}$, only the small splitting of 0.043 mT could be established with certainty. HMO–McLachlan calculations suggest that it should be attributed to the four tetrazine N centres. Other hyperfine coupling constants may amount to multiples of this value. Unfortunately, it was not possible to obtain ENDOR spectra due to insufficient saturation in the media necessary. The lower *g* value at 2.0024 also confirms the single occupation of the b_{1u} orbital with its not exclusive localization of π spin density at nitrogen centres. The lower spin-orbit coupling constants of carbon π centres in relation to corresponding N atoms cause less deviation of *g* from the free electron value.

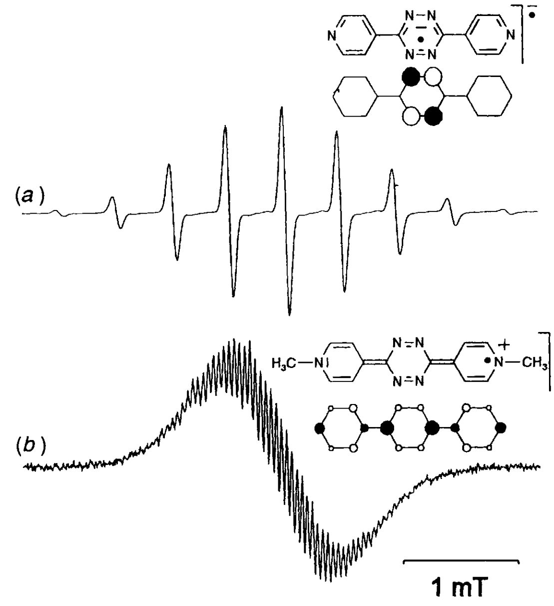

Fig. 3 EPR spectra at room temperature of (*a*) $4\text{-bptz}^{\bullet -}$ generated by electrochemical reduction in DMF–0.1 mol dm^{-3} Bu_4NPF_6 and of (*b*) $Me_2(4\text{-bptz})^{\bullet +}$ obtained *via* reduction with thallium in DMF

Summarizing, it turns out that an orbital change of the SOMO can be effected for the 4-bptz system albeit only with strong electrophiles coordinated to the pyridyl nitrogen sites.

UV–VIS absorption spectroscopy

Although the EPR data have already unambiguously answered the question of the SOMO characters in the reduced dap and 4-bptz species we sought additional evidence for our assignments from absorption spectroscopy. Most radical ions, especially those of unsaturated N-heterocycles, are distinguished by characteristic long wavelength absorption bands which involve transitions to or from the SOMO.[14,15]

The situation is most clear-cut in the case of the 4-bptz systems. The typical feature of the non-reduced species 4-bptz and R_2bptz^{2+} is the weak n→π* transition of the tetrazine ring at *ca.* 525 nm. In the bis(pentacarbonyltungsten) complex, this feature is obscured by the expected[12] ligand-field (LF, d→d)

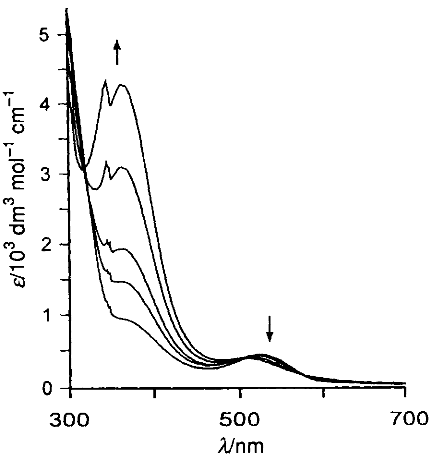

Fig. 4 UV–VIS spectroelectrochemistry of 4-bptz$^{0/\bullet-}$ in DMF–0.1 mol dm^{-3} Bu$_4$NPF$_6$

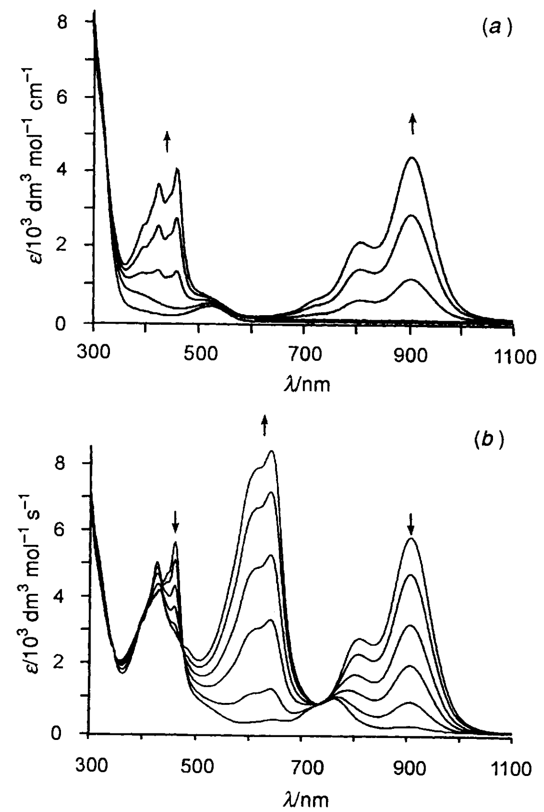

Fig. 5 UV–VIS–NIR spectroelectrochemistry of Me$_2$(4-bptz)$^{2+/\bullet+/0}$ in DMF–0.1 mol dm^{-3} Bu$_4$NPF$_6$. (*a*) Reduction of Me$_2$(4-bptz)$^{2+}$ to Me$_2$(4-bptz)$^{\bullet+}$ and (*b*) reduction of Me$_2$(4-bptz)$^{\bullet+}$ to Me$_2$(4-bptz)^0.

band at 400 nm and a solvatochromic metal-to-ligand charge transfer (MLCT) transition which lies between 430 nm (in DMF) and 514 nm (in toluene). The relatively high energy of the observable MLCT transition for this dinuclear W(0) complex with an easily reduced ligand must be attributed to an 'MLCT2' transition d→π*(b$_{1u}$). The lower lying a$_u$ MO has no orbital coefficients at the coordination site (the 'metal–ligand interface') and the low energy 'MLCT1' transitions d→π*(a$_u$) are not observed within the tailing of the MLCT2 band. The complex (4-bptz)[W(CO)$_5$]$_2$ is thus a typical system where 'redox (or EPR) orbitals' and 'optical orbitals' are different.[16] No emission was observed for this complex at 283 K in toluene, either because of the special LUMO/SLUMO situation or other effects of efficient quenching. The related (4-apy)[W(CO)$_5$]$_2$, where 4-apy is the 4,4'-azobis(pyridine) ligand, with a single low-lying b$_g$ MO [3a] and an MLCT absorption maximum at 582 nm in toluene exhibits weak emission at λ > 755 nm from an MLCT excited state under the same circumstances.[12d]

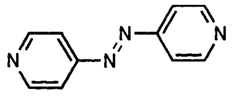

4-apy

Reduction of the various 4-bptz compounds produces quite differing results (Table 2). In the visible region, the spectroelectrochemically generated radical anion 4-bptz$^{\bullet-}$ of the parent compound shows only a slightly shifted and broadened band which, according to INDO/S calculations, involves n→π* and SOMO→SLUMO (a$_u$→b$_{2g}$) transitions of low intensity (Fig. 4, Table 2). A similar broad band is observed at somewhat longer wavelengths for the reduced ditungsten(0) complex. In contrast to typical radical anion complexes,[17] the observable MLCT band is not affected here by reduction because the added electron goes into the a$_u$ MO whereas the intense MLCT feature involves the b$_{1u}$ orbital.

The one-electron reduced form Me$_2$(4-bptz)$^{\bullet+}$, on the other hand, produces the typical spectrum of a methylviologen-type radical cation:[11a,b,15] an intense absorption with vibrational structuring ($\Delta\nu$ = 1325 cm^{-1}) occurs in the near IR region (Fig. 5). The long wavelength shift is in full agreement with an empirical rule [eqn. (2)] given by Hünig and Berneth for the

$$\lambda_{\max}{}^{(\bullet+)} = (kN) + b \qquad (2)$$

absorption energy of radical intermediates of coupled bis(*N*-methyl-4-pyridyl) redox systems.[11a] This rule predicts $\lambda_{\max}$ = 927 nm [*N* is the number of π electrons within the shortest distance of the end groups (in this case 13), k = 72.50 and b = -15.16 (for *N*-methyl-4-pyridyl)[11a]] for a derivative bridged by an aromatic ring, which is apparently a good model for the *s*-tetrazine bridged species.

Other transitions of Me$_2$(4-bptz)$^{\bullet+}$ are well reproduced by the INDO/S calculations (Table 2), the presence of the main transition in the near IR region causes this radical intermediate to have only a pale yellow colour. The facile and reversible second reduction of this system allowed us to obtain spectroelectrochemical information also for the neutral form, Me$_2$(4-bptz), which is intensely blue due to an allowed transition at *ca.* 640 nm (Fig. 5, Table 2). The Me$_2$(4-bptz)$^{n+}$ redox system thus shows just the opposite colour effects as the prototypical methylviologen system where the radical intermediate is intensely blue and the doubly reduced (neutral) form is yellow–orange.[11a]

In any case, the contrasting spectroelectrochemical behaviour (Fig. 4) as well as the EPR results (Fig. 3) illustrate the radically different character of the singly occupied MOs for 4-bptz$^{\bullet-}$ and its ditungsten(0) complex on one side (^{2}A$_u$ species) and the dialkylated derivatives R$_2$(4-bptz)$^{\bullet+}$ with their ^{2}B$_{1u}$ ground state on the other side. As their structures suggest, this dichotomy should also imply a very different capacity for π conjugation and different rotation barriers around the aryl–aryl bonds; such effects will be studied further.

The absorption spectra of dap and Me$_2$dap^{2+} in the near UV–VIS region can be readily interpreted (Table 2).[11b] All calculations (HMO, AM1, INDO/S) suggest that the vibrationally structured long wavelength band systems of both dap and Me$_2$dap^{2+} are caused by transitions from the π HOMO (b$_{3g}$) to the b$_{1u}$ orbital which, however, is only the second lowest unoccupied MO in dap, as suggested by the EPR of dap$^{\bullet-}$.[4a] The HOMO→LUMO (b$_{3g}$→a$_u$) transition of dap lies at higher energy (Table 2).

In addition to the intense π→π* transitions, the new bis(pentacarbonyltungsten) complex of dap exhibits the

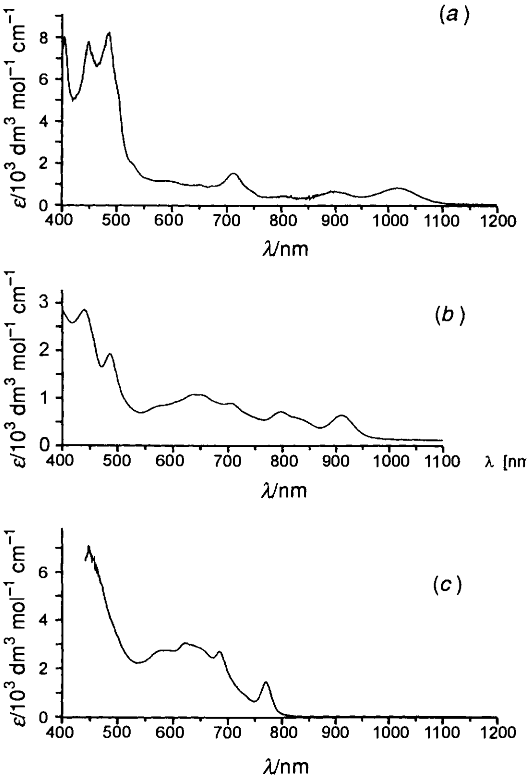

Fig. 6 Absorption spectra of (*a*) cathodically generated dap$^{\bullet -}$ in THF–0.1 mol dm^{-3} Bu_4NPF_6, (*b*) potassium-generated (dap$^{\bullet -}$)-$[W(CO)_5]_2$ in THF and (*c*) $Me_2dap^{\bullet +}$ in acetonitrile, as obtained by reduction of the precursor with thallium metal

familiar[12] LF and MLCT features, the high energy of the latter being due to the just moderate π acceptor capacity of the ligand. As the EPR results have already indicated, the electronic structure of the complex is similar to that of (bp)-$[W(CO)_5]_2$.[12,13] This correspondence extends not only to the absorption features and to the well known negative solvatochromism of the MLCT band,[12b] but also to the emission of (dap)$[W(CO)_5]_2$ in fluid solution after excitation at 380 nm. Whereas the free ligand emits strongly at 460 nm with further weak shoulders at 480 and 510 nm (in CH_2Cl_2), the main broad emission band of the dinuclear complex lies at 585 nm with a shoulder at *ca.* 630 nm. These features are shifted to longer wavelengths by *ca.* 10 nm in the more polar benzonitrile which further suggests that this luminescence may be attributed to emission from two MLCT excited states.[12c] Excitation spectra of (dap)$[W(CO)_5]_2$ based on the 580 nm luminescence yield maxima at 452 nm with a weak long wavelength shoulder and a more pronounced shoulder at *ca.* 400 nm. These data clearly support the assignments made above and are compatible with the b_{1u} MO as lowest π* orbital in the complex as opposed to the situation in the free ligand.

Fig. 6 shows the VIS–NIR absorption spectra of the radical species dap$^{\bullet -}$, (dap$^{\bullet -}$)$[W(CO)_5]_2$ and $Me_2dap^{\bullet +}$. An absorption spectrum of photogenerated $Me_2dap^{\bullet +}$ in aqueous medium has been published earlier.[4b]

Although the contrast between the spectra is not as striking as in the case of the 4-bptz analogues, there is clearly a closer correspondence between the spectra of (dap$^{\bullet -}$)$[W(CO)_5]_2$ and $Me_2dap^{\bullet +}$ as opposed to that of free dap$^{\bullet -}$. The latter exhibits a vibrationally structured ($\Delta\nu$ = 1275 cm^{-1}) band system in the near IR region which is attributed to the $a_u \rightarrow b_{2g}$ (SOMO→SLUMO) transition and which occurs similarly at 1020 nm in the pyrene radical anion.[14] Other major absorption maxima appear correspondingly at 712 nm (pyrene anion[14] and dap$^{\bullet -}$) as $a_u \rightarrow b_{2g}$ (SOMO→FLUMO) transitions and at 492 nm (pyrene anion[14]) or 486 nm (dap$^{\bullet -}$) as $b_{3g} \rightarrow a_u$ (HOMO→SOMO) transitions.

On the other hand, the absorption spectra of the radicals (dap$^{\bullet -}$)$[W(CO)_5]_2$ and $Me_2dap^{\bullet +}$ look more like 'methylviologen radical' spectra[11a,18] with their typical broad, structured hump at *ca.* 630 nm. In addition, there are long wavelength features at 911 nm (ditungsten complex) and 771 nm (dialkylated radical) which can be attributed to $b_{1u} \rightarrow b_{2g}$ (SOMO→FLUMO) transitions. In all cases, the SOMO→LUMO, *i.e.* the $a_u \rightarrow b_{1u}$ or $b_{1u} \rightarrow a_u$ transitions are not observed, either due to low intensity (u→u transitions) and/or their occurrence at very long wavelengths.

Two-electron reduction was possible for Me_2dap^{2+} to give a purple neutral species Me_2dap^0 with quinonoid structure. The main long wavelength absorption band at 563 nm is attributed to the b_{1u} (HOMO)→b_{2g} (SLUMO) transition.

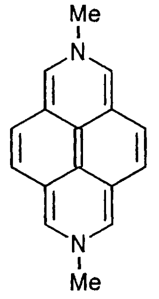

Me_2dap

Acknowledgements

This work was supported by Deutsche Forschungsgemeinschaft (Germany, SFB 329 and collaboration grants), the Academy of Sciences of the Czech Republic, the Foundation for Research Development (South Africa) and by an Alexander von Humboldt Fellowship (to M. M. Z.). M. M. Z. also thanks the University of Zululand for granting a sabbatical leave.

References

1 (*a*) A. Streitwieser, Jr., *Molecular Orbital Theory for Organic Chemists*, Wiley, New York, 1961; (*b*) E. Heilbronner and H. Bock, *The HMO-Model and its Application*, Wiley/Verlag Chemie, London/Weinheim, 1976; (*c*) J. N. Murrell, *The Theory of the Electronic Spectra of Organic Molecules*, Methuen, London, 1963.

2 (*a*) W. Kaim, *J. Am. Chem. Soc.*, 1982, **104**, 3833 and refs. cited therein; (*b*) S. Ernst, C. Vogler, A. Klein, W. Kaim and S. Zalis, *Inorg. Chem.*, 1996, **35**, 1295; (*c*) A. Klein, W. Kaim, E. Waldhör and H.-D. Hausen, *J. Chem. Soc., Perkin Trans. 2*, 1995, 2121.

3 (*a*) W. Kaim and S. Kohlmann, *Inorg. Chem.*, 1990, **29**, 1898; (*b*) W. Kaim and J. Fees, *Z. Naturforsch., Teil B*, 1995, **50**, 123.

4 (*a*) J. Bruhin and F. Gerson, *Helv. Chim. Acta*, 1975, **58**, 2422; (*b*) A. J. Blacker, J. Jazwinski and J.-M. Lehn, *Helv. Chim. Acta*, 1987, **70**, 1.

5 S. Hünig, J. Gross, E. F. Lier and H. Quast, *Liebigs Ann. Chem.*, 1973, 339.

6 (*a*) W. Kaim, S. Ernst and V. Kasack, *J. Am. Chem. Soc.*, 1990, **112**, 173; (*b*) M. Krejcik, M. Danek and F. Hartl, *J. Electroanal. Chem. Interfacial Electrochem.*, 1987, **222**, 161.

7 (*a*) GAUSSIAN 92/DFT, Revision G.3, M. J. Frisch, G. W. Trucks, H. B. Schlegel, P. M. W. Gill, B. G. Johnson, M. W. Wong, J. B. Foresman, M. A. Robb, M. Head-Gordon, E. S. Replogle, R. Gomperts, J. L. Andres, K. Raghavachari, J. S. Binkley, C. Gonzalez, R. L. Martin, D. J. Fox, D. J. Defrees, J. Baker, J. J. P. Stewart and J. A. Pople, Gaussian Inc., Pittsburgh (PA), 1993; (*b*) M. J. S. Dewar, E. G. Zoebisch, E. F. Healy and J. J. P. Stewart, *J. Am. Chem. Soc.*, 1985, **107**, 3902; (*c*) M. J. S. Dewar and W. Thiel, *J. Am. Chem. Soc.*, 1977, **99**, 4899; 4907; (*d*) J. Ridley and M. C. Zerner, *Theoret. Chim. Acta*, 1973, **32**, 111.

8 (*a*) F. Gerson, *High Resolution E.S.R. Spectroscopy*, Wiley/Verlag Chemie, London/Weinheim, 1970; (*b*) A. D. McLachlan, *Mol. Phys.*, 1960, **3**, 233.

9 A. Ioffe, A. Ayalon and M. Rabinovitz, *J. Chem. Soc., Perkin Trans. 2*, 1994, 1115.

10 (*a*) F. Bertinotti, G. Giacomello and A. Liquori, *Acta Crystallogr.*,

1956, **8**, 513; (*b*) W. Kaim, M. Moscherosch, S. Kohlmann, J. S. Field and D. Fenske, in *The Chemistry of the Copper and Zinc Triads*, eds. A. J. Welch and S. K. Chapman, Royal Society of Chemistry, Cambridge, 1993, p. 248; (*c*) S. Kohlmann, Ph.D. Thesis, University of Frankfurt, 1988.

11 (*a*) S. Hünig and H. Berneth, *Top. Curr. Chem.*, 1980, **92**, 1; (*b*) S. Hünig, J. Gross, E. F. Lier and H. Quast, *Liebigs Ann. Chem.*, 1973, 339; (*c*) T. Troll, *Electrochim. Acta*, 1982, **27**, 1311; (*d*) J. Poppe, M. Moscherosch and W. Kaim, *Inorg. Chem.*, 1993, **32**, 2640.

12 (*a*) M. M. Zulu and A. J. Lees, *Inorg. Chem.*, 1988, **27**, 1139; (*b*) M. M. Zulu and A. J. Lees, *Inorg. Chem.*, 1988, **27**, 3325; (*c*) M. M. Zulu and A. J. Lees, *Inorg. Chem.*, 1989, **28**, 85; (*d*) M. M. Zulu, A. J. Lees, W. Kaim and S. Kohlmann, unpublished results.

13 (*a*) W. Kaim, *Inorg. Chim. Acta*, 1981, **53**, L15; (*b*) W. Kaim, *Chem. Ber.*, 1982, **115**, 91; (*c*) W. Kaim, *J. Organomet. Chem.*, 1984, **262**, 171.

14 T. Shida, *Electronic Absorption Spectra of Radical Ions*, Elsevier, Amsterdam, 1988.

15 (*a*) P. S. Braterman and J.-I. Song, *J. Org. Chem.*, 1991, **56**, 4678; (*b*) M. Krejcik, S. Zalis, M. Ladwig, W. Matheis and W. Kaim, *J. Chem. Soc., Perkin Trans. 2*, 1992, 2007; (*c*) W. Kaim, A. Schulz, F. Hilgers, H.-D. Hausen, M. Moscherosch, A. Lichtblau, J. Jordanov, E. Roth and S. Zalis, *Res. Chem. Intermed.*, 1993, **19**, 603.

16 (*a*) F. Barigelletti, A. Juris, V. Balzani, P. Belser and A. von Zelewsky, *Inorg. Chem.*, 1987, **26**, 4115; (*b*) E. Amouyal, A. Homsi, J. C. Chambron and J. P. Sauvage, *J. Chem. Soc., Dalton Trans.*, 1990, 1841; (*c*) J. Fees, W. Kaim, M. Moscherosch, W. Matheis, J. Klima, M. Krejcik and S. Zalis, *Inorg. Chem.*, 1993, **32**, 166.

17 (*a*) W. Kaim and S. Kohlmann, *Inorg. Chem.*, 1990, **29**, 2909; (*b*) P. S. Braterman, J.-I. Song, S. Kohlmann, C. Vogler and W. Kaim, *J. Organomet. Chem.*, 1991, **411**, 207.

18 W. Kaim and W. Matheis, *Chem. Ber.*, 1990, **123**, 1323.

Paper 5/05404D
Received 11*th August* 1995
Accepted 24*th January* 1996